MDPI

Article

BN Diamane-like Quasicrystal Based on 30° Twisted H-BN Bilayers and Its Approximants: Features of the Atomic Structure and Electronic Properties

Leonid A. Chernozatonskii [1,2,*] **and Aleksey I. Kochaev** [1,3,*]

1 Emanuel Institute of Biochemical Physics RAS, 4 Kosygin Street, 119334 Moscow, Russia
2 Scientific School on Chemistry and Technology of Polymer Materials, Plekhanov Russian University of Economics, 117997 Moscow, Russia
3 Research and Education Center "Silicon and Carbon Nanotechnologies", Ulyanovsk State University, 42 Leo Tolstoy Street, 432017 Ulyanovsk, Russia
* Correspondence: chernol-43@mail.ru (L.A.C.); a.kochaev@ulsu.ru (A.I.K.)

Abstract: The dodecagonal graphene quasicrystal (GQC) based on a 30° twisted bigraphene has been well investigated. Recently, the sp^3-hybridizated carbon analog, the diamane quasicrystal as a H(F) functionalized GQC was proposed. Here we present a study of a similar sp^3-hybridizated boron nitride 3-fold symmetry piezoelectric quasicrystal (BNnQC) based on a 30° twisted hexagonal BN bilayer (BNQC). The analysis of the atomic and electronic structures of its approximants based on 29.4° and 27.8° twisted h-BN bilayers has been carried by using of the density functional theory (DFT). The calculated values of the energy gaps ~5 eV classify this predicted boron nitride material as a new wide-gap 2D quasicrystal.

Keywords: 2D quasicrystals; boron nitrides; twisted bilayers; DFT modeling; electronic properties

1. Introduction

Since the discovery of quasicrystals based on rapidly solidified Al86Mn14 alloys [1] there has been a wide variety of not only 3D, but also 2D quasicrystals [2]. Various structures of long-range aperiodic order 2D materials have been obtained and are currently being studied, including graphene quasicrystal (GQC) formed from 30° twisted bigraphene [3,4]. Wide-gap super-hard QC [5] formed by functionalized GQC and belonging to the Moiré diamond family has recently been proposed and investigated for energy stability. These proposed films, as well as their predecessors, 2D diamond-like sp^3-hybridized carbon materials, called diamanes [5–7], are functionalized untwisted layers of graphene with interlayer covalent bonds, with a bandgap of E_g ~3 eV, and unique mechanical properties. Only in 2020 were details on the successful synthesis of fluorinated [8] and hydrogenated diamanes [9] published. Earlier attempts led to the formation of another diamane-like material: diamandoids [10], one-side OH− or H passivated few graphene layers and diamondenes transformed from bigraphenes to 2D diamond films by pressure and temperature treatment [11–13]. Moiré diamanes based on twisted bigraphene were also studied as the next variety of diamanes. They can have a wide range of energy gaps [14] and thermal conductivity [15], which depends on the twisted angle and numbers of adsorbed atoms.

Today, hexagonal boron nitride (h-BN) monolayers are widely researched and implemented in practical applications [16]. Having non-conductive electrical properties, h-BN monolayers are a good platform for collecting other 2D materials, tubes or fullerenes. It is shown [17] that vertical heterostructures of graphene and boron nitride with rotation angles of 10.9° and 25.3° are stable compounds of a Moiré type. Recently diamond-like structures based on bilayers of hexagonal nitrides [18,19] have been theoretically studied too. The obtained infrared and Raman spectra will facilitate the experimental detection of

bornitranes with a rotation angle of 21.8° [19]. Herein, we consider features of a similar structure formed by H-absorption on 30° twisted h-BN bilayers, as an example of long-range aperiodic order 2D sp^3-boronnitridane quasicrystal (BNnQC). A structural analysis in accordance with the electronic properties for large-scale BN quasicrystal approximants is presented. We consider also the structure of a boron-nitridene quasicrystal (BNenQC), which can be formed from 30° twisted h-BN bilayers under high pressures and temperatures similar to the well-known diamondene. These quasicrystals with 3-fold symmetry must be piezoelectric.

The introduction of "twisted" planar materials into 2D electronics, including various piezo, photo, opto, and nonlinear functioning devices is very promising [20], and the production of sufficiently wide layers is quite consistent with the capabilities of modern nanotechnologies [21]. Therefore, the study of new QCs of the diamane-like type, intended to aid in the advancement of the above fields, is also promising. As follows from the review [20], the preparation of the layers with controlled growth and high-quality and scalable synthesis is now not difficult, especially with the development of CVD technologies, methods, and devices for creating rotated layers with an accuracy of 0.1°.

2. Computational Methodology

The construction and visualization of the structural and volumetric data were carried out using the free VESTA (ver. 3.5.8) software [22]. We computed and compared the following 2D structures: h-BN (B2N2), BNn27.8 (B26N26H30), BNn29.4 (B194N194H174), BNenQC disk (B348, N348), and BNnQC disk (B348, N348, H396). The numbers in front of the letters indicate the number of corresponding atoms in a unit cell or cluster. To study the structural and electronic properties of the considered approximants of BNnQC, we used ab initio simulations, based on the density functional theory (DFT) as implemented in the licensed QuantumATK code (ver. 2021.06) [23]. The generalized gradient approximation (GGA) for the exchange and correlation potential expressed by the Perdew−Burke−Ernzerhof (PBE) functional and the projector augmented wave potential (PAW) are used in our calculations [24]. All calculations were carried out using periodic boundary conditions. The all structures are optimized, while the Hellman–Feynman force convergence exceeded 10^{-2} eV/Å. To neglect the influence of the boundary conditions in the z-direction perpendicular to the sheet, we take the value of the cell parameter along z equal to 15 Å. The van der Waals interaction was taken into account using the DFT-D2 method of Grimme [25]. The use of these approaches has previously made it possible to predict entire families of 2D materials [26].

3. Results and Discussion

3.1. Atomic Structure of 2D Diamane-like BN Quasicrystal

The appearance of Moiré bilayer structures with a suitable (in particular, hexagonal) cell requires fine tuning of the angle of rotation between the two layers. The Moiré patterns underlying the known Moiré bilayer structures occur at a rotation angle close to 30°. Such angles lead to structures that are described by elementary cells with sizes that are quite accessible for analysis by modern quantum chemistry software [23].

Usually, 2D quasicrystals based on two twisted 30° hexagonal layers are described in frame of the Stampfli scheme [2–5,27]. This scheme is the perfect 2D one atomic 12-fold symmetry quasicrystal lattice without thickness, as a mosaic of squares and triangles with identical scales. We consider for a twisted 30° hexagonal bimodal BN layer structure the same mosaic scheme of squares (s-tiles) and triangles (t-tiles), as shown in Figure 1a, taking into account the two main atomic elements of h-BN and 3D geometry of its real thickness (Figure 1b). This 3-fold symmetry quasicrystal structure differs from the 6-fold symmetry of the DnQC [15], with new atomic structural "color" tile mosaics on the plane (Figures 1 and 2) because of the distinguishable atomic placement in the sp^3-hybridized atomic structure. So, H (or F, OH) absorption can be realized on two sides of the 30° twisted h-BN layers turning them into a diamane-like quasicrystal.
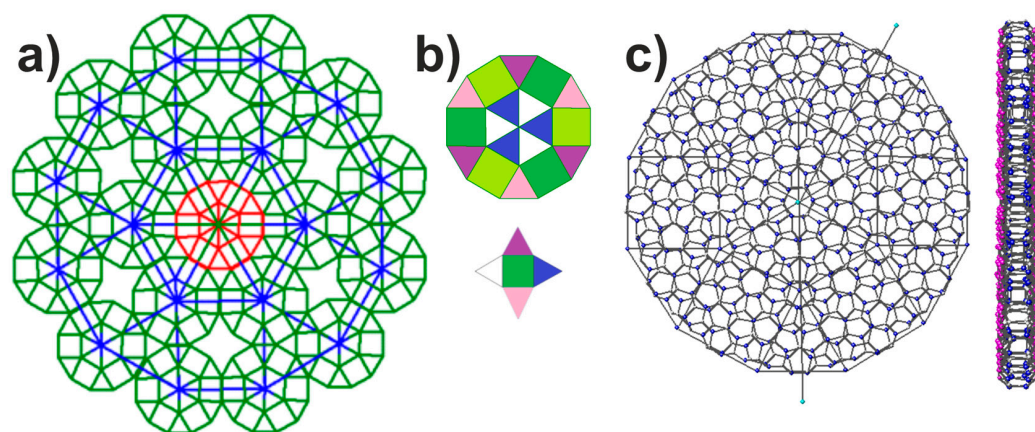
Figure 1. (**a**) The Stampfli dodecagonal quasiperiodic lattice with main disk element consisting of 6 squares and 12 triangles, with the scale parameter L_0 (red) in the center and the 1st inflation lattice enlarged $2 + \sqrt{3}$ times (blue lines); (**b**) filled with color tiles from the main disk element and a space between the 4 disks in a 3-fold symmetry retransformed Stampfli scheme; (**c**) top view of the corresponding BNnQC atomic distribution (atoms: B—yellow, N—blue, H—white) and side view with H atoms adsorbed by violet B and N atoms. At the connection nodes of the squares and triangles there are always "rings" of twisted 30° BN hexagons.
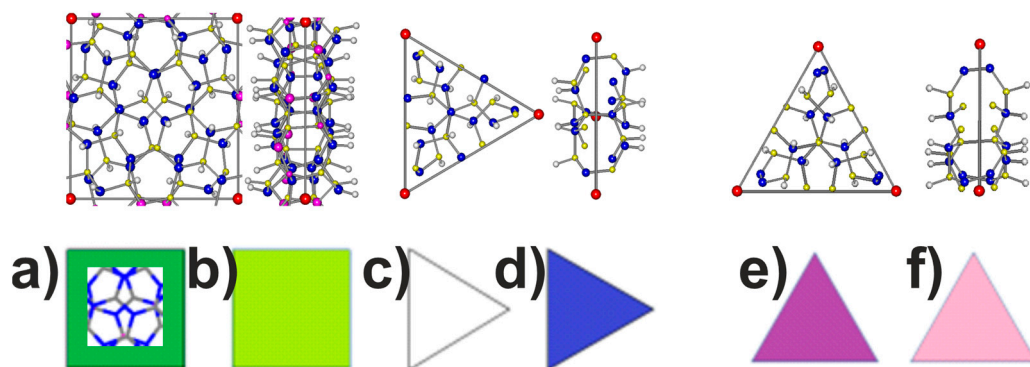

Figure 2. Atomic top and side view of the corresponding atomic distribution in BNnQC tiles, upper row (atoms: B—yellow, N—blue, H—white; atomic "cross" element for the preferred absorption places of the two H-pairs is shown in the green tile (**a**)) and the color tiles on the lower row: a square with the front and back sides ((green—(**a**), and light green—(**b**))), both white and blue triangles (**c**,**d**) correspond to the front and back sides of the atomic t_1-triangle with covalent B-N' and B'-N pairs in the angles (upper view), the violet triangle (**e**) corresponds to the t_2 triangle with covalent coupled N-N' pairs in the angles (upper atomic view), and the rose t_3-triangle (**f**) with coupled B-B' pairs in the angles (its atomic structure equivalent to the previous t_2-triangle tiling with reversed B and N atoms is not shown).

Note that in the same Stampfli lattice with square and triangle tiles, the DnQC will consist of triangular and square double-sided tiles. In this case, the QC structure itself has a 6-fold symmetry axis; the main disk consists of six identical triangles assembled in the center, six identical squares and identical triangles, but differing from the "center" triangles by the atomic structure on their front and back sides.

3.2. The Building Blocks of the 2D Structure Assembled with the Reconstructed Stampfli Tiling

We consider the ideal picture of the possible filling of the two BNQC surfaces with adsorbents of those B and N atoms that are at the smallest distance from the atoms of the neighboring layer (Figure 1c). The preferred sites for the adsorption of atoms by nearby B and N atoms in neighboring layers are "bond crosses", following the description of the

picture of optimal H absorption during the formation of similar Moiré diamanes [14,28]. The greater vibration freedom of these B-N and B'-N' pairs along the h-BN bilayer normal facilitates the simultaneous adsorption of H atom pairs by them and the formation of complexes (H-B-N-H and H'-B'-N'-H') in "cross" places, see the upper row and square inset in Figure 2a.

So, the obtained 3-fold symmetry quasicrystal structure has to describe the frame of the new reconstructed Stampfli scheme (RS) with "color" tiles taking into account their atomic structure and lowering the symmetry of the BNnQC itself to 3-fold symmetry (Figures 1 and 2). Because of this, compared to the tiling in a DQC mosaic [15], we have to increase the number of square and triangle elements in the plane Stampfli scheme up to six (see below row in Figure 2). To simplify the description of the mosaic, we consider the front and back sides of the triangle "(e)" or "(f)" to be equally shaded, since in the atomic structure of the BNnQC the main role is played by the meeting points of the tiles, where these tiles "enter" at the corners with the same atom pairs (see Figure 2e,f).

The RS tiling schemes for the BN quasicrystal built from equilateral triangles is shown in Figure 3. The self-similar form of the first next generation tiling inflation is also shown nearby as a self-similar filling of the translucent squares and triangles on a $2 + \sqrt{3}$ longer length scale.
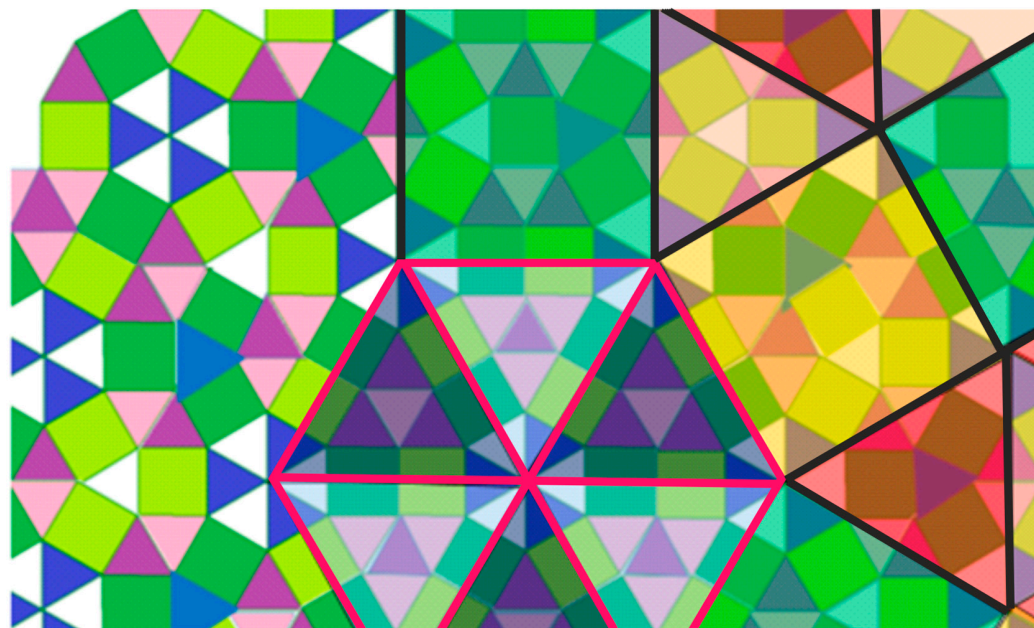

Figure 3. Retransformed Stampfli color scheme with scale parameter of L_0 for 2 types of s-tiles and 4 types of t-tiles. The right part is the 1st inflation of the RS scheme picture with translucent tiles with a size of $L_1 = (2 + \sqrt{3})L_0$ (the nodes are located in the center of the nodes in the main RS scheme).

With a non-ideal pattern of adatom attachment (even with a change in the number of adsorbent atoms in the square and triangular RS tiles), in general, the adsorption sites around the rings at the RS lattice sites (meeting points of the square and triangle corners) will retain approximately the same order as is the case when considering the ideal structures of Moiré diamanes. The structures and properties of such a quasicrystal with defects mostly in the structures of the ideal triangles and squares, as shown in Figure 3, after real adhesion requires separate consideration. However, we believe that the pattern of filling such a TS lattice with "rings" at the meeting points of even partially defective triangle and square "tiles", will basically have the same form as shown in Figure 1. Such a conclusion, of course, must be confirmed by electron diffraction patterns from actual synthesized BNnQC structures, as is always conducted in the same cases during the identification of quasicrystals [1–4,29].

3.3. BNn29.4 and BNn27.8 Approximants

As a rule [5], either periodic structures or large atomic clusters act as approximants of 2D quasicrystal. Usually, the diffraction pattern and properties of the 2D QC are estimated by constructing a diffraction pattern from an approximant; a periodic structure which is closest to the QC atomic structure [1–4]. Similarly, to the previously discussed DnQC, ab initio computations of its atomic and electronic structures were carried out by using the closest to 30° B-nitridanes, namely BNn29.4 and BNn27.8, as approximants with density of atoms per square and covalent bonds similar to BNnQC. Figure 4 shows that the unit cell of the BNn29.4 approximant containing all types of RS tiles of the quasicrystal BNnQC and the approximant BNn27.8 unit cell consists of two triangles corresponding to the views of the tiles t_1 shown in Figure 2c,d, which is the same as in the center of the main RS color disk element in Figure 1b.
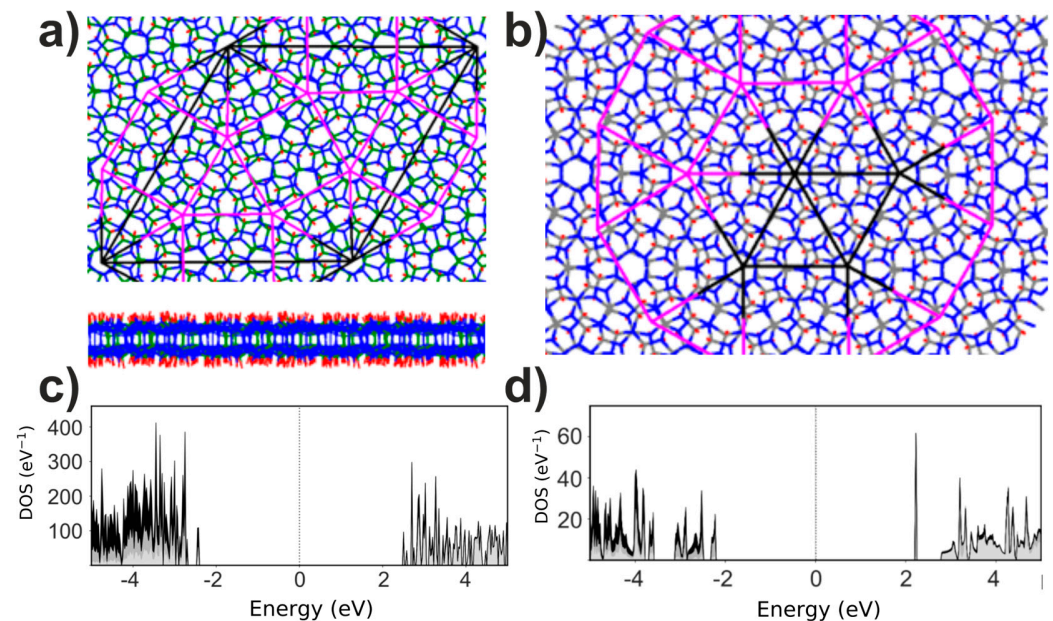

Figure 4. (**a**) Approximants of BNnQC: top and side views of the BNn29.4 atomic structure (H—white, B—green, N—blue, black unit cell with parameter L = 25.2 Å); (**b**) top view of BNn27.8 (black unit cell with parameter L = 9.19 Å); (**c,d**) electronic density of states (DOS) of these approximants. Violet lines mark Stampfli lattice disks.

The calculation of the formation energy E_f of the considered approximants showed a small difference in its values (only 0.03 eV/(BN atoms)), similar difference E_f energies for Moiré diamanes Dn29.4 and Dn27.8 [14], i.e., such energetically stable Moiré B-nitridane approximants indicate the stability of the BNn quasicrystal.

The bond lengths (Å) of the approximants are not the same and are within the limits: $d_{BH,NH}$ = 1.2–1.3, 1.02–1.05 and $d_{BN,BB,NN}$ = 1.4–1.7, 1.3–2.2, 1.6–2.3. The calculated bond length values are in good agreement with the values obtained for the non-Moiré and Moiré bilayers of boron nitride [19]. From Figure 4c,d, it follows that B-nitrane BNn29.4 has a wide bandgap E_g of 4.9 eV and B-nitrane BNn27.8 has a bandgap of 4.4 eV. Localized states are found at the bandgap boundaries of BNn29.4: one DOS peak is located below the continuous part of the valence band at δv = 0.3 eV, another peak is located in the upper continuous part of the conduction band at δc = 0.3 eV. There are similar local peaks in the DOS picture for BNn27.8. Accounting for these features leads to the estimate of the gaps at the boundary of the continuous zones of $\Delta = E_g + \delta v + \delta c$, which are equal to 5.4 eV for BNn29.4 and 5.1 eV for BNn27.8. These values are close to the energy gap of the 3D crystal cubic BN, but are different from the values typical for AB and AA′ bornitranes [19]. This confirms our assumptions about the wide dielectric gap of BNnQC

itself. The resonant nature of the electronic spectrum indicates its manifestations in the study of the optoelectronic properties of the considered quasicrystal.

The near 30° twisted bilayer graphene was used as the basis for the Moiré diamane-like materials [14,15]. The Moiré atomic structure is more complicated than untwisted 2D structures and also contains a lot of non-equivalent atoms and interlayer bonds. This feature leads to an increase in the high bandgap and stiffness constants [15,16], and a reduction of thermal conductivity in comparison with the AB-diamane [18]. Similar properties should also appear for the BNnQC and its approximants, since their atomic structure also contains many non-equivalent atoms and interatomic bonds (see Figures 1c and 3a).

Unfortunately, commensurate Moiré approximants with angles closest to 30° have larger calculated cell sizes and a higher number of atoms in them, which makes it difficult to calculate their optimal atomic structures and properties. However, the approximants with twisted angles at 29.4° and 27.8° are a good tool for such assessments, for estimation of the properties of the BNnQC. Similar calculations for the DnQC approximants [14] and 2D oxides QC [29], served to substantiate the features of the atomic and electronic structures of these quasicrystals.

Note that the unit cell in the BNn27.8 structure consists of two triangles [14] with a structure that almost coincides with the two triangles in the center of the main disk element RS scheme of the BNnQC (BNn30). Thus, the BNnQC mosaic can be considered to be composed in a rather complex way of triangle and square elements from the unit cells of the commensurate bilayer structures twisted at angles of 29.4° and 27.8° (see Figure 4). Such a quasi-amorphous structure should have a very ultralow thermal conductivity, as occurs in the Dn27.8 Moiré diamane [15].

It is natural to expect that passivation of the H, F or OH groups only on one side of the 30° h-BN bilayer placed on a substrate will lead to the formation of 2D sp^3 boron-nitridene quasicrystal like Moiré diamanes [30].

3.4. Boron-Nitridene Quasicrystal

It is known that under high pressure and temperature, the structure of a graphene bilayer turns into a layer containing a sp^3-hybrid pair of atoms from neighboring layers [11–13]. Under the same impact the 30° twisted hexagonal BN bilayer (BNQC), as well as its approximants, should be transformed into diamondene-like structures, where the "cross" pairs of atoms standing in the neighboring layers at the closest distance will remain in the sp^2-hybrid state, while the others will be transformed into covalently bonded pairs of sp^3 atoms. The latter can be called QC nitridones (BNonQC). The scheme of a color mosaic composed of triangular and square two-sided tiles of a different structure remains in the form of a transformed RS mosaic for all layers with a diatomic hexagonal lattice (even for a molecular QC with a twisted 30° angle free from adsorbed H or F atoms).

As an example, we modeled similar 2D symbiotic sp^2-sp^3 structures, BNenQC and BNen27.8 (Figure 5a), named B-nitridenes by analogy with diamondenes [11]. We believe that at pressures in the same range used in experiments [11–13], not only for twisted bigraphenes but also twisted h-BN bilayers, transformation into such sp^2-sp^3 structures will occur. Obviously, BNonQC, like all untwisted and twisted diamonds, can only be obtained on a substrate. However, in this case, it will be more difficult to calculate its properties, which already depend on this substrate, than the properties of the DnQC (and even more so the BNnQC structures). This large layer of work requires a separate study with an enumeration of all the possible substrates.
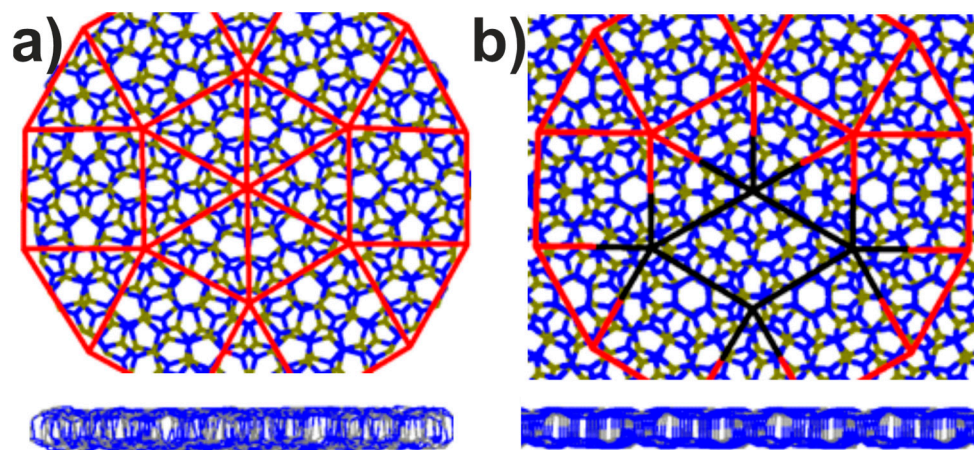
Figure 5. Top and side views of the atomic representations of B-nitridenes (red lines denote Stampfli scheme disk, B—yellow and N—blue atoms): BNenQC quasicrystal based on a 30° twisted h-BN bilayer (**a**), and a BNen27.8 (black block is unit cell) based on a 27.8° twisted h-BN bilayer (**b**).

4. Conclusions

We have studied one of the ideal options for connecting pairs of B and N atoms in transformed Stampfli scheme tiles of a quasicrystal. For example, in the corners of all the triangles that are included in the nodes of the RS lattice, B-N', B-B, and N-N' bonds are covalently connected. However, under certain conditions in the absorption process, hydrogen can also sit on these atoms, breaking their bonds. This will correspond to the inclusion of defects in the ideal picture of the arrangement of the atoms in the tiles of the RS scheme. Such "defective" QCs, which we believe will generally preserve the geometry of the RT lattice, require special studies with sufficiently large arrays of atoms and computational procedures. Studies on the mechanical properties and phonon spectra of even the considered approximants will also require more computer calculations and will be carried out later.

Due to the bonds of atomic pairs are disordered with respect to the normal to the film (Figure 1c), this BNnQD structure looks like a quasi-amorphous material, in contrast to the well-observed period of Moiré nitridane (see Figure 5). Such BNnQC quasicrystal should, like its closest "relative" diamane quasicrystal, have high hardness, and ultralow thermal conductivity and friction. Since the bonds between the B (N) and F atoms are stronger than with hydrogen, the F-BNnQD has to have an ultra-weak wearable surface. All BNn quasicrystal structures do not have an inversion center, therefore they are piezoelectric. The latter opens up the possibility of their use in mechano-electrical nanodevices. It has been previously shown [31,32] that perforation and functionalization of classical 2D materials can lead to piezoelectric moduli that are much higher than those for lithium niobate.

The considered quasicrystalline structures will be of interest from the point of view of studies and applications of their high "sliding" properties due to the rough surface [33]. This can be especially pronounced if, instead of hydrogen, the adsorption of fluorine is used, which attaches to the surface of the bilayer more strongly than hydrogen.

Since the closest crystal to diamond in hardness is BN, it is logical to assume that the BNnQC will also be close in hardness to the 3D cubic BN. Resonant DOS for the considered BN structures should lead to resonant optical and optoelectronic effects, which will also find application in new nanodevices. We hope that the considered B-nitride quasicrystals (based on twisted 30° hexagonal two atomic unit cell AlN, GaN layers et al.) can be created using the same methods previously used in the modern twist technique for creating 30° bilayers and obtaining diamanes [8–13].

References

1. Shechtman, D.; Blech, I.; Gratias, D.; Cahn, J.W. Metallic Phase with Long-Range Orientational Order and No Translational Symmetry. *Phys. Rev. Lett.* **1984**, *53*, 1951–1953. [CrossRef]
2. Yadav, T.P.; Kumbhakar, P.; Mukhopadhyay, N.K.; Galvao, D.S.; Ajayan, P.M.; Ranganathan, S.; Chattopadhyay, K.; SekharTiwary, C. Revisiting Quasicrystals for the Synthesis of 2D Metals. *Trans. Indian Inst. Met.* **2022**, *75*, 1093–1100. [CrossRef]
3. Ahn, S.J.; Moon, P.; Kim, T.-H.; Kim, H.-W.; Shin, H.-C.; Kim, E.H.; Cha, H.W.; Kahng, S.-J.; Kim, P.; Koshino, M.; et al. Dirac electrons in a dodecagonal graphene quasicrystal. *Science* **2018**, *361*, 782–786. [CrossRef] [PubMed]
4. Yao, W.; Wang, E.; Zhang, Y.; Zhang, J.R.; Chan, C.K.; Chen, C.; Avila, J.; Asensio, M.C.; Zhu, J.; Zhou, S. Quasicrystalline 30° twisted bilayer graphene as an incommensurate superlattice with strong interlayer coupling. *Proc. Natl. Acad. Sci. USA* **2018**, *115*, 6. [CrossRef]
5. Chernozatonskii, L.A.; Demin, V.A.; Kvashnin, A.G.; Kvashnin, D.G. Diamane quasicrystals. *Appl. Surf. Sci.* **2022**, *572*, 151362. [CrossRef]
6. Chernozatonskii, L.A.; Sorokin, P.B.; Kvashnin, A.G.; Kvashnin, D.G. Diamond-like C2H nanolayer, diamane: Simulation of the structure and properties. *JETP Lett.* **2009**, *90*, 134–138. [CrossRef]
7. Chernozatonskii, L.A.; Demin, V.A.; Kvashnin, D.G. Fully Hydrogenated and Fluorinated Bigraphenes–Diamanes: Theoretical and Experimental Studies. *J. Carbon Res.* **2021**, *7*, 17. [CrossRef]
8. Bakharev, P.V.; Huang, M.; Saxena, M.; Lee, S.W.; Joo, S.H.; Park, S.O.; Dong, J.; Camacho-Mojica, D.C.; Jin, S.; Kwon, Y.; et al. Chemically Induced Transformation of Chemical Vapour Deposition Grown Bilayer Graphene into Fluorinated Single-Layer Diamond. *Nat. Nanotechnol.* **2020**, *15*, 59–66. [CrossRef]
9. Piazza, F.; Cruz, K.; Monthioux, M.; Puech, P.; Gerber, I. Raman Evidence for the Successful Synthesis of Diamane. *Carbon* **2020**, *169*, 129–133. [CrossRef]
10. Barboza, A.P.M.; Guimaraes, M.H.D.; Massote, D.V.P.; Campos, L.C.; Neto, N.M.B.; Cancado, L.G.; Lacerda, R.G.; Chacham, H.; Mazzoni, M.S.C.; Neves, B.R.A. Room-Temperature Compression-Induced Diamondization of Few-Layer Graphene. *Adv. Mater.* **2011**, *23*, 3014–3017. [CrossRef]
11. Gao, Y.; Cao, T.; Cellini, F.; Berger, C.; de Heer, W.A.; Tosatti, E.; Riedo, E.; Bongiorno, A. Ultrahard carbon film from epitaxial two-layer graphene. *Nat. Nanotech.* **2018**, *13*, 133–138. [CrossRef]
12. Ke, F.; Zhang, L.; Chen, Y.; Yin, K.; Wang, C.; Tzeng, Y.-K.; Lin, Y.; Dong, H.; Liu, Z.; Tse, J.S.; et al. Synthesis of Atomically Thin Hexagonal Diamond with Compression. *Nano Lett.* **2020**, *20*, 5916–5921. [CrossRef] [PubMed]
13. Cellini, F.; Lavini, F.; Cao, T.; de Heer, W.; Berger, C.; Bongiorno, A.; Riedo, E. Epitaxial Two-Layer Graphene under Pressure: Diamene Stiffer than Diamond. *FlatChem* **2018**, *10*, 8–13. [CrossRef]
14. Chernozatonskii, L.A.; Demin, V.A.; Kvashnin, D.G. Ultrawide-bandgap Moiré diamanes based on bigraphenes with the twist angles Θ∼ 30°. *Appl. Phys. Lett.* **2020**, *117*, 253104. [CrossRef]
15. Chowdhury, S.; Demin, V.A.; Chernozatonskii, L.A.; Kvashnin, D.G. Ultra-Low Thermal Conductivity of Moiré Diamanes. *Membranes* **2022**, *12*, 925. [CrossRef] [PubMed]
16. Angizi, S.; Alem, S.A.A.; Azar, M.H.; Shayeganfar, F.; Manning, M.I.; Hatamie, A.; Pakdel, A.; Simchi, A. A comprehensive review on planar boron nitride nanomaterials: From 2D nanosheets towards 0D quantum dots. *Prog. Mater. Sci.* **2022**, *124*, 100884. [CrossRef]
17. Demin, V.; Chernozatonskii, L. Diamane-like Films Based on Twisted G/BN Bilayers: DFT: Modelling of Atomic Structures and Electronic Properties. *Nanomaterials* **2023**, *13*, 841. [CrossRef]
18. Zhang, Z.; Zeng, X.C.; Guo, W. Fluorinating Hexagonal Boron Nitride into Diamond-Like Nanofilms with Tunable Band Gap and Ferromagnetism. *J. Am. Chem. Soc.* **2011**, *133*, 14831–14838. [CrossRef]

19. Chernozatonskii, L.A.; Katin, K.P.; Kochaev, A.I.; Maslov, M.M. Moiré and non-twisted sp^3-hybridized structures based on hexagonal boron nitride bilayers: Ab initio insight into infrared and Raman spectra, bands structures and mechanical properties. *Appl. Surf. Sci.* **2022**, *606*, 154909. [CrossRef]

20. Han, Z.; Zhang, R.; Li, M.; Li, L.; Geng, D.; Hu, W. Recent advances in the controlled chemical vapor deposition growth of bilayer 2D single crystals. *J. Mater. Chem. C* **2022**, *10*, 13324. [CrossRef]

21. Kim, S.M.; Hsu, A.; Park, M.H.; Chae, S.H.; Yun, S.J.; Lee, J.S.; Cho, D.H.; Fang, W.; Lee, C.; Palacios, T.; et al. Synthesis of large-area multilayer hexagonal boron nitride for high material performance. *Nat. Commun.* **2015**, *6*, 8662. [CrossRef] [PubMed]

22. Momma, K.; Izumi, F. VESTA: A Three-Dimensional Visualization System for Electronic and Structural Analysis. *J. Appl. Crystallogr.* **2008**, *41*, 653–658. [CrossRef]

23. Smidstrup, S.; Markussen, T.; Vancraeyveld, P.; Wellendorff, J.; Schneider, J.; Gunst, T.; Verstichel, B.; Stradi, D.; Khomyakov, P.A.; Vej-Hansen, U.G.; et al. QuantumATK: An integrated platform of electronic and atomic-scale modelling tools. *J. Phys. Cond. Mat.* **2019**, *32*, 015901. [CrossRef] [PubMed]

24. Perdew, J.P.; Burke, K.; Ernzerhof, M. Generalized Gradient Approximation Made Simple. *Phys. Rev. Lett.* **1996**, *77*, 3865. [CrossRef] [PubMed]

25. Grimme, S. Semiempirical GGA-type density functional constructed with a long-range dispersion correction. *J. Comput. Chem.* **2006**, *27*, 1787–1799. [CrossRef]

26. Kochaev, A.I. Hypothetical planar and nanotubular crystalline structures with five interatomic bonds of Kepler nets type. *AIP Adv.* **2017**, *7*, 025202. [CrossRef]

27. Stampfli, P. A Dodecagonal Quasiperiodic Lattice in Two Dimensions. *Helv. Phys. Acta* **1986**, *56*, 1260–1263.

28. Chernozatonskii, L.A.; Katin, K.P.; Demin, V.A.; Maslov, M.M. Moiré diamanes based on the hydrogenated or fluorinated twisted bigraphene: The features of atomic and electronic structures, Raman and infrared spectra. *Appl. Surf. Sci.* **2021**, *537*, 148011. [CrossRef]

29. Schenk, S.; Krahn, O.; Cockayne, E.; Meyerheim, H.L. 2D honeycomb transformation into dodecagonal quasicrystals driven by electrostatic forces. *Nat. Commun.* **2022**, *13*, 7542. [CrossRef]

30. Chernozatonskii, L.A.; Demin, V.A.; Kvashnin, D.G. Moiré Diamones: New Diamond-like Films of Semifunctionalized Twisted Graphene Layers. *J. Phys. Chem. Lett.* **2022**, *13*, 5399–5404. [CrossRef]

31. Brazhe, R.; Kochaev, A.; Sovetkin, A. Piezoelectric Effect in Graphene-Like 2D Supracrystals with a Periodic Perforation Breaking the Central Symmetry. *Phys. Solid State* **2013**, *55*, 1925. [CrossRef]

32. Brazhe, R.; Kochaev, A.; Sovetkin, A. Piezoelectric Effect in Fluorographane-Like 2D Supracrystals. *Phys. Solid State* **2013**, *55*, 2094. [CrossRef]

33. Leconte, N.; Park, Y.; An, J.; Jung, J. Commensuration torques and lubricity in double Moire systems. *arXiv* **2023**, arXiv:2301.04105.